Clinical & Experimental Metastasis (2025) 42:20
https://doi.org/10.1007/s10585-025-10337-2

RESEARCH PAPER

Brain metastases lung adenocarcinoma patients with BRG1 loss have a grim prognosis, featuring unique morphological and methylation characteristics

Junjie Yang[1] · Jing Feng[1] · Zejun Duan[1] · Xing Liu[2] · Hongwei Zhang[1] · Mingshan Zhang[1] · Zhong Ma[1] · Zejuan Hu[1] · Lei Xiang[1] · Xueling Qi[1]

Received: 11 December 2024 / Accepted: 12 March 2025

Abstract

BRG1 deficiency in patients with lung adenocarcinoma that has metastasized to the brain, termed BRG1-deficient brain metastasis lung adenocarcinoma, is an uncommon event. Prior to this study, these patients had not undergone extensive molecular and (epi)genetic analysis. We report a comprehensive clinical, histopathologic, and molecular assessment of 9 BRG1-deficient brain metastasis lung adenocarcinoma cohort (BRG1-deficient BM cohort) in comparison with a 16 BRG1-retained brain metastasis lung adenocarcinoma cohort (BRG1-retained BM cohort). Patients with BRG1-deficient BM exhibited a significantly increased risk of mortality. Molecular analysis revealed a high prevalence of mutations in SMARCA4 and TP53 genes within this group. DNA methylation molecular diagnostics showed a high rate of genomic instability and a markedly lower DNA methylation age in these patients. Functional enrichment analysis of differentially methylated genes suggested that hypomethylation genes were primarily associated with the negative regulation of neuron differentiation, G protein-coupled receptor signaling pathways, and cell differentiation. Conversely, hypermethylation was linked to the regulation of small GTPase mediated signal transduction, Rho protein signal transduction, DNA damage response, and apoptotic processes. This study investigated a rare subgroup of lung adenocarcinoma patients with brain metastasis characterized by BRG1 deficiency and a poor prognosis. Our study not only provides a comprehensive multi-omic data resource but also provides valuable biological insights into patients. The findings may serve as a valuable reference for the future pathological diagnosis of BRG1-deficient brain metastasis in lung adenocarcinoma patients.

Keywords BRG1-deficient · Lung adenocarcinoma · Brain metastatic · Immunohistochemistry · DNA methylation

Introduction

BRG1, encoded by the SMARCA4 gene, is one of the most common anomalous ATP-dependent catalytic subunits of the SWI/SNF chromatin-remodeling complexes, participating in the activation or repression of transcriptional processes in various types of cancer [1, 2]. BRG1 deficient case accounts for ~10% of non-small cell lung cancer (NSCLC) patients and associates with NSCLC progression and poor prognosis [3]. Recently, several newly published studies have demonstrated the direct impact of SMARCA4 deficiency on SWI/SNF complex function and chromatin regulation that induces aggressive malignancy during lung cancer development [3]. Likewise, SMARCA4 is also involved in regulating cytoskeletal function [2]. Non-small cell lung cancer studies based on previously published data have shown that SMARCA4-deficient NSCLC has highly aggressive behavior with vascular invasion and pleural metastasis [4, 5]. A subset of SMARCA4-deficient transformed cells impaired the function of the SWI/SNF complex and reduced the chromatin accessibility of lung-specific transcription factors, which induced specific lung stem cells to undergo malignant

Junjie Yang and Jing Feng contributed equally to this work.

✉ Xueling Qi
xszqxl169@mail.ccmu.edu.cn

[1] Department of Pathology, Sanbo Brain Hospital, Capital Medical University, Xiangshan Yikesong 50, Haidian District, Beijing 100093, China

[2] Department of Neurosurgery, Capital Medical University, Beijing 100070, China

Published online: 21 March 2025

transformation, resulting in an advanced dedifferentiated tumor state as well as tumor progression and metastasis. A study of TCGA data further confirmed that SMARCA4-mutant lung adenocarcinoma (LUAD) also exhibits a highly dedifferentiated state like relevant mouse models [6].

Brain metastases from primary solid organ cancers are the most common central nervous system (CNS) tumors [7]. Of these, the most common primary tumor is lung cancer [8]. Unfortunately, treatment options for LUAD-BM are limited and generally less effective than those for primary LUAD patients [9]. Morphologic features and molecular mechanism of BRG1 deficiency in LUAD with brain metastases have rarely been reported. Accurate diagnosis and treatment options for BRG1 deficiency LUAD with brain metastases are few and limited in their efficacy.

DNA methylation profile has emerged as a diagnostic and prognostic assay for molecular classification of solid cancers including brain tumors [10], sarcomas [11], meningiomas, and sinonasal carcinomas [12]. Previous studies have compared DNA methylation signatures to categorize clinically relevant subgroups in NSCLC [13], and DNA methylation has been proposed as a prognostic tool to predict early recurrence in stage I LUAD tumors [14, 15]. However, methylation typing diagnosis for brain metastases from lung adenocarcinoma is currently unexplored.

We conducted an in-depth investigation of 25 cases of lung adenocarcinoma brain metastasis based on the status of the BRG1 protein. For the first time, we identified a subset of lung adenocarcinoma brain metastasis with significant poor prognosis characterized by BRG1 deficiency. On the basis of clinical pathological diagnosis and DNA methylation molecular diagnosis, these patients had a high frequency of genomic instability and significantly lower DNA methylation age. Further analysis of the molecular characteristics of this group of patients also indicated that they had a high frequency of mutations in the SMARCA4 and TP53 genes, and shared similar genomic mutation characteristics of malignant tumors as SMARCA4 deficiency NSCLC.

Materials and methods

Patient cohort

Nine patients diagnosed with lung adenocarcinoma brain metastases with BRG1 deficiency were included in this study, of which eight were collected from Sanbo Brain Hospital, Capital Medical University and one from Beijing Neurosurgical Institute, Capital Medical University. All cases had a clear BRG1 staining result and a history of lung occupancy or lung cancer. All of LUAD-BM cases without BRG1 deficiency ($N=16$) and non-tumor brain tissues ($N=7$) for comparing were collected at Sanbo Brain Hospital, Capital Medical University. The non-tumor brain tissues were collected from patients with traumatic brain injury who underwent microsurgery, including: fetal hypoxia, neonatal cerebral infarction, viral encephalitis, trauma from falling, cerebral hemorrhage, trauma from falling, and brain tissue scars after trauma. The pathology staining slides were evaluated by two independent neuropathologists. Clinical data were obtained from medical records.

Histology and immunohistochemical staining

Four- to five-µm sections were cutting from formalin-fixed paraffin-embedded (FFPE) tissue specimens for hematoxylin and eosin (H&E) and immunohistochemistry (IHC) according to manufactures´ instructions of the respective reagents. The staining results were independently reviewed by two neuropathologists. Immunohistochemical staining was performed on FFPE sections with the primary antibodies described below and the respective secondary antibodies matching the primary antibodies. The immunohistochemical staining makers included: (i) markers localized to the nucleus: BRG1 (ZSGB-BIO, ZA-0673), TTF1 (ZSGB-BIO, ZM-0250), Ki-67 (ZSGB-BIO, ZM-0167); (ii) markers localized to the cytoplasm: NapsinA (ZSGB-BIO, ZM-0417), Cytokeratin (CK) (JIN QIAO YA TU, GC-0343), Cytokeratin 7 (CK7) (ZSGB-BIO, ZM-0071), Cytokeratin 19 (CK19) (ZSGB-BIO, ZM-0074). All reagents purchased were in working solution concentrations.

DNA sequence analysis

For the formalin-fixed paraffin-embedded samples, ten 5 µm tumor slices were used for DNA extraction using the QIAamp DNA FFPE Kit (QIAGEN, Valencia, CA, USA) following the manufacturer's instructions. DNA quality was assessed by spectrophotometry with absorbance at 230,260, and 280 nm, and quantified by Qubit 2.0. Libraries were prepared as previously reported [16]. Briefly, 1 µg of fragmented genomic DNA underwent t end-repairing, a-tailing, and ligation with indexed adapters sequentially, followed by size selection using Agencourt AMPure XP beads (Beckman Coulter). Hybridization-based target enrichment was carried out with GeneseeqOne™ pan-cancer gene panel (494-cancer-relevant genes, Nanjing Geneseeq Technology Inc.) (Table S4), only one sample with 139-lung-cancer-relevant gene panel (Nanjing Geneseeq Technology Inc.). Captured libraries by Dynabeads M-270 (Life Technologies) were amplified in KAPA HiFi HotStart ReadyMix (KAPA Biosystems) and quantified by qPCR using the KAPA Library Quantification kit (KAPA Biosystems). Target-enriched libraries were sequenced on the HiSeq4000 platform

(Illumina) with 2 × 150 bp pair-end reads. Sequencing data were demultiplexed by bcl2fastq (v2.19), analyzed by Trimmomatic [17] to remove low-quality (quality < 15) or N bases, and mapped to the reference hg19 genome (Human Genome version 19) using the Burrows-Wheeler Aligner [18]. PCR duplicates were removed by Picard (available at: https://broadinstitute.github.io/picard/). The Genome Analysis Toolkit (GATK) [19] was used to perform local realignments around indels and base quality reassurance. SNPs and indels were called by VarScan2[20] and HaplotypeCaller/UnifiedGenotyper in GATK, with the mutant allele frequency (MAF) cutoff as 0.5% for tissue samples and a minimum of three unique mutant reads. Common variants were removed using dbSNP and the 1000 Genome project. Gene fusions were identified by FACTERA [21] and allele-specific CNVs were analyzed by FACETS [22] with a 0.2 drift cut-off for unstable joint segments.

DNA methylation profiling preprocess

To explore the DNA methylation profiles of LUAD-BM tumors, DNA methylation was assessed using the Illumina Infinium Human Methylation 850 (850k) BeadChip (Illumina, San Diego, USA). The cohort included nine BRG1-deficient BM cohort samples and eight samples of BRG1-retained BM cohort. The samples with available methylation sequencing data were detailed in Supplemental Table S1. First, DNA was extracted from FFPE samples using ReliaPrep FFPE gDNA Miniprep Kit (Promega, WI, Germany), and then restored using Illumina HD FFPE Restoration Kit (Illumina, CA, USA) according to the manufacturer's instructions. Second, DNA underwent bisulfite conversion, amplification, fragmentation, and hybridization to the 850 K BeadChip (Illumina, CA, USA) following the manufacturer's protocols. The raw data preprocessing and normalization were performed using the minfi package [23], and samples with a detection ratio of CpG sites (detection p-value < 0.05) greater than 95% were used for subsequent analysis. Exclusion of probes according to previous reporting criteria [24]. beta and M values were calculated. Then, MethylCIBERSORT and Epidish [25, 26] were applied to predict the tumor purity. The sample with an average purity of less than 0.3 from the results of the two algorithms will be excluded in following analysis. As a result, four samples were excluded due to low tumor purity.

Unsupervised clustering analysis

Unsupervised hierarchical clustering in our cohort using the 10,000 most variably methylation probes, were performed and visualized using R package pheatmap (v1.0.12), and the Pearson correlation coefficient was the distance measure. The t-stochastic neighbor embedding (t-SNE) analysis was performed with the Rtsne package (v0.17) in R 4.0 with default parameters.

DNAm age analysis

DNAm age was calculated using the Horvath clock, which is a multi-tissue age predictor that estimates DNAm age by automatically selecting a set of 353 CpG probes by an elastic net regression model [27]. Beta values for our cohort were obtained from the raw IDATs, and quantile normalization was applied. Sex probes were removed. SNPs were filtered using using the dropLociWithSnps function from the minfi package. The final matrix of beta values for all the samples was passed as input for the Horvath clock to generate the DNAm age for each sample.

Identification of differentially methylated positions

The differentially methylated positions (DMPs) were predicted using the R package ChAMP (v.2.24) [28]. Only probes with Benjamini-Hochberg adjusted $P < 0.01$ and|deltaBeta| >0.2 would be identified as DMPs. The DMPs mapped at promoter regions (including TSS1500, TSS200, 5'UTR, and 1st exon) were kept in gene ontology (GO) analysis. The GO functional annotation analysis was performed using the DAVID website (https://david.ncifcrf.gov/)[29].

Copy number variation analysis

Genome-wide DNA methylation array data was also used to assess copy number variation (CNVs). The non-tumor brain tissue (NTB) samples were used as a control. The raw intensities (idat files) of every single sample were first analyzed separately with the "conumee" R package (v.1.32.0) (http://bioconductor.org/packages/conumee/) [30] by default parameters, the segment files were generated. To obtain cumulated CNVs per group, the R package GenVisR (v.1.31.1) [31] was used to process segment files, which can generate plots displaying the proportion of copy number losses/gains at a group level.

Statistical significance analysis

Statistical analyses were conducted using IBM SPSS Statistics 19 (http://esd2.spss.com). Chi [2] test and Mann-Whitney test were used to find associations between clinical and molecular data. For survival analysis, we used the Kaplan-Meier method, overall survival (OS) was calculated from the date of surgical resection to the date of death or the date of last follow-up. In the significant difference analysis, ns.

presented not significant, * presented $p<0.05$, ** presented $p<0.01$, *** presented $p<0.001$.

Results

The clinical characteristics of brain-metastatic lung adenocarcinoma with BRG1 deficiency

Due to the low frequency of BRG1-deficiency, we only collected 9 samples of BRG1-deficient brain metastases (BM) from lung adenocarcinoma in our routine pathology bank, named BRG1-deficient BM cohort for convenience. To better distinguish the clinical features of BRG1-deficient brain metastases from lung adenocarcinoma, we also collected the samples of BRG1-retained brain metastases from lung adenocarcinoma, including 16 patients, named BRG1-retained BM cohort. In the BRG1-deficient BM cohort, patients' ages ranged from 37 to 73 years, with a median age of 60.8 years and a male-to-female ratio of 8:1. (Table 1 and Supplemental Table S1). However, in BRG1-retained BM cohort, there were 6 men and 10 women, ranging in age from 48 to 79 years (median age, 61.1 years) (Table 1 and Supplemental Table S1). 55.6% of BRG1-deficient BM cohort had a significant smoking history of >15 pack-years. The smoking status of only 2 patient was unknown. In the BRG1-retained BM cohort, only 25% of the patients had a history of smoking more than 15 pack-years (Table 1). BRG1-deficient BM cohort was significantly associated with male sex and smoking history. Patients tend to exhibit symptoms that are predominantly associated with a single lesion. The duration of disease in this group is relatively short, ranging from 0.5 to 13 months (median 2.78 months). However, in the BRG1-retained BM cohort, this group of patients had a relatively long duration of illness ranging from 0.25 to 120 months (median 19.77 months) (Table 1). In the BRG1-deficient BM cohort, patients' symptoms started with intracranial symptoms, including dizziness, headache, limb weakness, blurred vision, and slurred speech. In the BRG1-retained BM cohort, patients started with pulmonary symptoms, including chest tightness, cough, and sputum (Supplemental Table S1). Thus, these two groups of patients show different clinical characteristics.

Table 1 Clinical features of BRG1-deficient BM cohort and BRG1-retained BM cohort

Variables	BRG1-deficient BM cohort ($N=9$)	BRG1-retained BM cohort ($N=16$)	*P* value
Age at diagnosis			0.44
Averge (min, Max)	60.8 (37–73)	61.1 (48–79)	
Sex number			0.02*
Female (%)	1 (11.1%)	10 (62.5%)	
Male (%)	8 (88.9%)	6 (37.5%)	
Smoking status			0.04*
Never smoker (%)	2 (22.2%)	12 (75%)	
>15 Pack-years (%)	5 (55.6%)	4 (25%)	
Missing (%)	2 (22.2%)	0	
Foci of disease			0.37
Unifocal (%)	6 (66.7%)	9 (56.3%)	
Multifocality (%)	3 (33.3%)	7 (43.7%)	
Course of disease			0.44
Average (min, Max)	2.78 (0.5–13)	19.77 (0.25–120)	

Different histologic pattern and IHC makers expression between BRG1-deficient BM cohort and BRG1-retained BM cohort

On histologic evaluation of the BRG1-deficient BM cohort, tumor cells were often arranged in solid, nested clusters or sheets. These structures were formed by segmenting vascular fibers and were characterized by cells that were obese, round, or cuboidal. However, glandular, tubular, or trabecular structures were rare. The cytoplasm of the cells was abundant and stained reddish, similar to the appearance of rhabdomyosarcoma. The nuclei were rounded or irregular with fine chromatin. The majority of samples exhibited large eosinophilic nuclei, and in some cases, scattered multinucleated or megakaryocytic cells were observed. (Fig. 1A). In the BRG1-retained BM cohort, the tumor cells were predominantly arranged in a ductal, papillary, or micropapillary pattern (Fig. 1E). These results indicate significant morphological variations between the two groups. Compared to BRG1-retained BM cohort, tumor cells in BRG1-deficient BM cohort exhibit more malignant characteristics.

The staining results of diagnosis-related markers play an important role in the diagnosis of pathology. All cases of BRG1-deficient BM group showed BRG1, TTF-1, and NapsinA immunohistochemical profiles of significant differences from the BRG1-retained BM cohort. In the BRG1-deficient BM group, immunohistochemical staining shows that BRG1 is absent along with the deletion of TTF1 and NapsinA (Fig. 1B-D; Table 2). In the other group, immunohistochemistry showed positive expression of TTF1, NapsinA, and no deletion of BRG1 (Fig. 1F-H; Table 2). The CK, CK7, and CK19 assays showed no significant differences between the two groups (Supplemental Fig. S1 and Table 2). CK7 reactivity was identified in 67% (6/9) of BRG1-deficient BM cohort and 100% (16/16) in the BRG1-retained BM cohort (Table 2). These results suggest that there was significant variability in the immunohistochemical profile of TTF-1, NapsinA, and BRG1 between the two groups of samples.

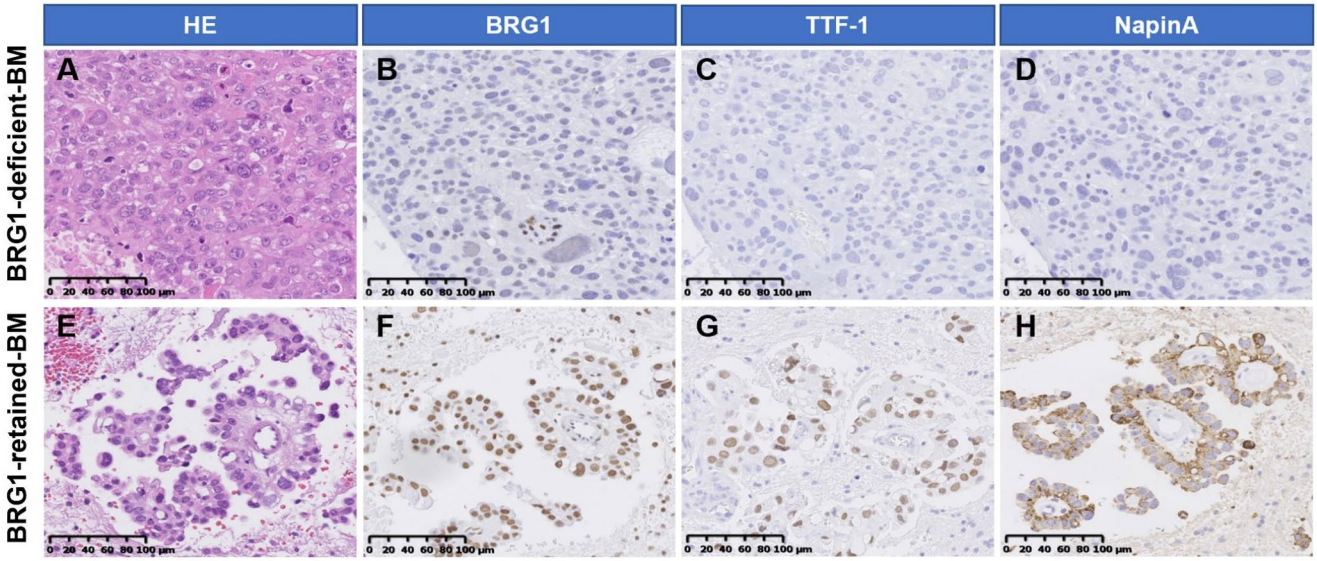

Fig. 1 The different and immunohistochemical characteristics of the between BRG1-deficient BM cohort and BRG1-retained BM cohort. The BRG1-deficient tumor cells were obese, round or rectangular, with abundant cytoplasm and red staining, similar to rhabdomyosarcoma (**A**), and the BRG1-retained tumor cells were predominantly arranged in a ductal, papillary, or micropapillary pattern (**E**). BRG1 expression was absent in the BRG1-deficient group along with the negative expression of TTF1 and NapsinA (**B-D**). In the BRG1-retained group, immunohistochemistry showed positive expression of TTF1, NapsinA, and BRG1 (**F-H**). Images of representative staining at a magnification of 200 x are shown. HE: indicates hematoxylin and eosin

Table 2 The different expression patterns of key IHC markers in BRG1-deficient BM cohort and BRG1-retained BM cohort

Immunomarker	BRG1-deficient BM cohort ($N=9$)	BRG1-retained BM cohort ($n=16$)
BRG1	0/9 (0)	16/16 (100%)
TTF1	1/9(11%)	14/16 (87.5%)
NapsinA	0/9(0)	15/16 (93.8%)
CK	9/9(100%)	16/16 (100%)
CK7	6/9 (67%)	16/16 (100%)
CK19	9/9 (100%)	16/16 (100%)
Ki67		
Low + intermediate	1 (12.5%)	6 (37.5%)
High	8 (87.5%)	10 (62.5%)

Ki67 high: Ki-67 positivity greater than 30%

BRG1-deficient BM cohort still with high frequency of SMARCA4 and TP53 mutation

The deletion of BRG1 expression was correlated with SMARCA4 mutation in NSCLC [32, 33]. Recent studies have revealed that NSCLC patients with SMARCA4 mutations, especially homozygous deletions and truncating mutations, were more likely to have drug resistance, early relapse, and poor clinical outcomes than patients with wild-type SMARCA4[34, 35]. Regarding the molecular characteristics in the BRG1-deficient BM cohort, we also found that 7/8 (87.5%) samples had SMARCA4 mutation (Fig. 2A). There were 4 SMARCA4 mutations categories: frameshift mutation ($n=4$, 50%), missense mutation ($n=1$, 12.5%), splice site mutation ($n=2$, 25%), missense & splice site mutation ($n=1$, 12.5%). Truncating mutation (i.e., frameshift mutations) constituted 37.5% of SMARCA4 mutations. The protein alterations include R192P, P222L, P311A, P305R, R414S and K587N (Fig. 2B).

We also found that all samples had TP53 mutation. The mutation types were missense mutation ($n=6$, 75%) and frameshift mutation ($n=1$, 12.5%). There was also one sample with copy number variations (Fig. 2A). The protein alterations include P72R, R110L, P151R, V157F, Y163C, and Y220C (Fig. 2C).

Co-mutations were also identified in other pan-cancer genes: LPR1B (62.5%), ROS1 (50%), PKHD1 (37.5%), NOTCH2 (37.5%), NCOR2 (37.5%), KMCT2D (37.5%), FAT1 (37.5%), CDKN2A (37.5%), ARID2 (37.5%) (Fig. 2A and Supplemental Table S2).

Using TCGA cohort, we also found three patients with lung adenocarcinoma brain metastasis who have SMARCA4 mutations. Two types of SAMRCA4 mutation were also found including a splice site mutation and a missense mutation (Supplemental Fig. S2A). TP53, STK11, KRAS, and CDKN2A mutations were also found in two samples (Supplemental Fig. S2B and Supplemental Table S2).

All the results illustrated that in the BRG1-deficient BM cohort, samples had high frequencies of mutations in SMARCA4 and TP53. These results indicate that the BRG1 deficiency malignant brain metastasis lung adenocarcinoma group also possesses the typical molecular characteristics of lung adenocarcinoma tumors.

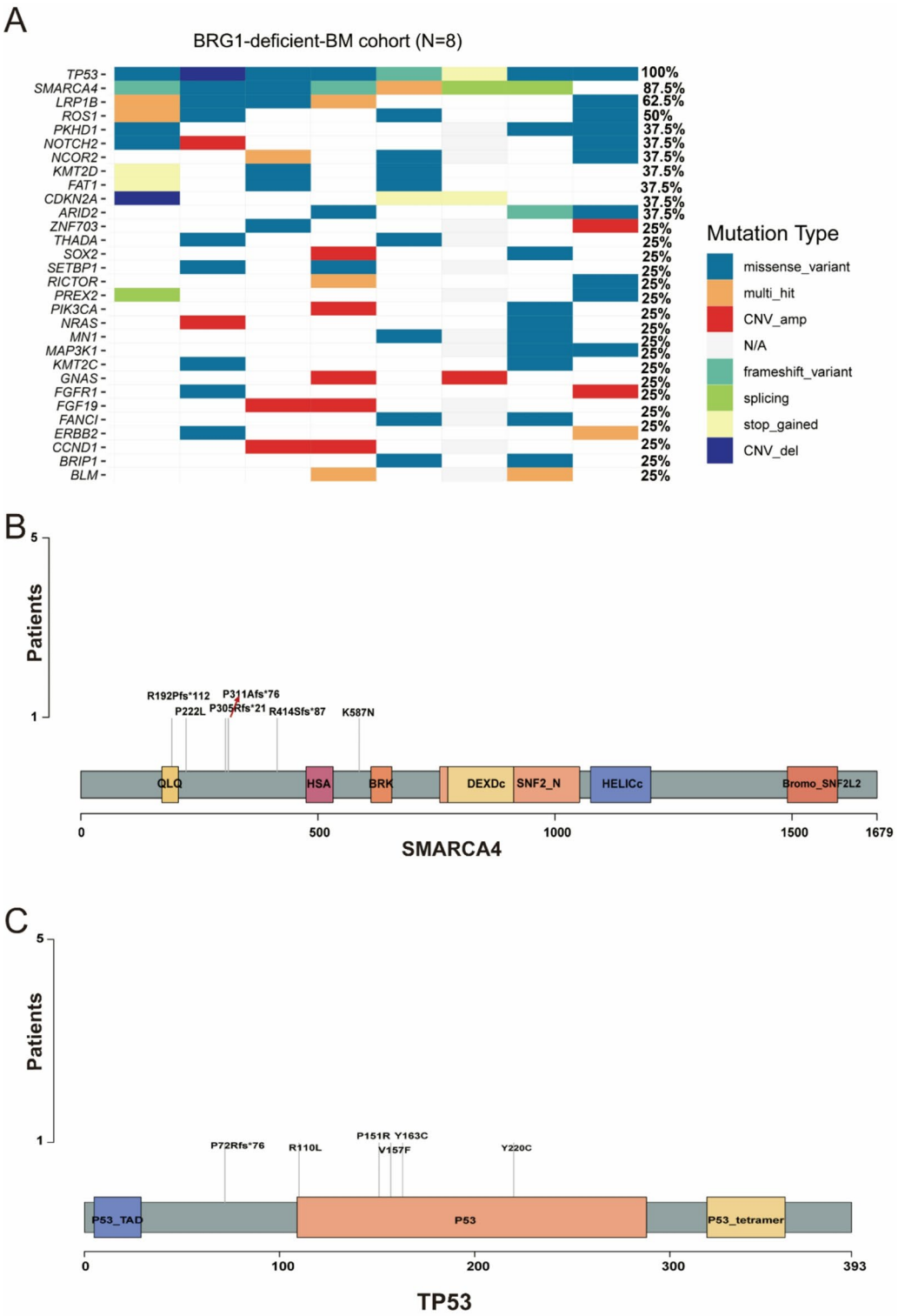

Fig. 2 Genetic alterations in BRG1-deficient BM cohort. (**A**) Genes co-altered in BRG1-deficient-BM group. Samples have high frequencies of mutations in SMARCA4 and TP53. (**B**) and (**C**) lollipop plot of SMARCA4 and TP53 alterations in BRG1-deficient BM cohort. SMARCA4: QLQ, Gln, Leu, Gln motif; HSA, helicase/SANT-associated domain; BRK: Brahma and Kismet domain; DEXDc, DEAD-like helicase superfamily domain; SNF2_N, SNF2 family N-terminal domain; HELICc, helicase superfamily C-terminal domain; Bromo_SNF2L2, bromodomain. TP53: P53_TAD: transactivation motif; P53: DNA-binding domain; P53_tetramer: P53 tetramerization motif. N/A: Not Available; Amp: amplification, Del: deletion

BRG1-deficient BM cohort with unique methylation characteristics and poorer prognosis

DNA methylation patterns in tumor cells or tissues can serve as powerful biomarkers for diagnosis, disease subclassification, patient stratification, and for predicting treatment responses [10, 12, 36, 37]. Molecular classification of tumors based on DNA methylation has proven to be a reliable tool. We performed genome-wide DNA methylation profiling in our cohort, DNA methylation array data of 17 samples passed quality control. And then 4 samples were excluded due to low tumor purity. Unsupervised Clustering Analysis of DNA methylation data was performed, both hierarchical clustering and T-SNE algorithms clustered samples in our cohort into two distinct groups. These two methylation groups corresponded exactly to the two previous subgroups based on BRG1 status (BRG1-deficient BM cohort and BRG1-retained BM cohort) (Fig. 3A and B). We assessed the impact of two clusters using the Kaplan-Meier method using the patients' clinical data. Overall survival (OS) was significantly different ($P<0.05$) between two subgroups. Compared with BRG1-retained BM cohort, patients in BRG1-deficient BM cohort had a significantly higher risk of death (Fig. 3C). These results indicate that the BRG1-deficient BM cohort, which has a poorer prognosis, possesses unique methylation characteristics.

BRG1-deficient BM cohort characterized by high-frequency genomic instability and low DNA methylation age

Acquired chromosomal instability, especially copy number variations (CNVs), has been considered an important determinant of cancer progression and clinical survival [38]. Genome-wide DNA methylation array data of LUAD-BM was also used to assess copy number variation (CNVs). In the BRG1-deficient BM cohort, high-frequency chromosome copy number changes were observed on chr4, chr5, chr6, chr9, and chr13 (Fig. 4A). In the BRG1-retained BM cohort, a high percentage of samples exclusively exhibited deletions on chr8p and amplifications on chr8q (Fig. 4B). Compared with the BRG1-retained BM cohort, the BRG1-deficient BM cohort had more genomic chromosomal copy number changes. This result illustrated that genomic instability may be correlated to the malignancy in the BRG1-deficient BM cohort.

The dramatic changes in DNA methylation may lead to chromosomal instability [39]. Another aspect of DNA methylation is its natural evolution during the individual's lifetime. Several studies have identified specific CpGs exhibiting age-related changes in the different tissues [40]. Such changes can be computed to provide a DNA methylation age (DNAm age) that estimates the "biological age" of tissues [27, 41]. Epigenetic age acceleration, which is the vertical shift between DNAm age and chronologic age, has been reported to be tightly associated with clinical outcomes of many diseases [42].Using the Horvath clock [27], the DNAm age was calculated for all 13 LUAD-BM tumors and 7 Non-tumor brain tissue. The BRG1-deficient BM cohort has a lower DNAm age compared with chronological age. There were no significant changes observed in the other two groups (Fig. 4C). Compared to non-tumor brain tissue and BRG1-retained BM cohort, BRG1-deficient BM cohort, which has a poorer prognosis, has significantly lower age acceleration ($p=0.0023$) (Fig. 4D). This result suggested that BRG1-deficient BM cohort with lower DNAm age has higher potential to proliferate and thus might grow into more aggressive tumors. Ki67 is an important indicator of the degree of tumor cell proliferation activity. Samples with Ki-67 positivity greater than 30% had 8 cases (8/9) in the

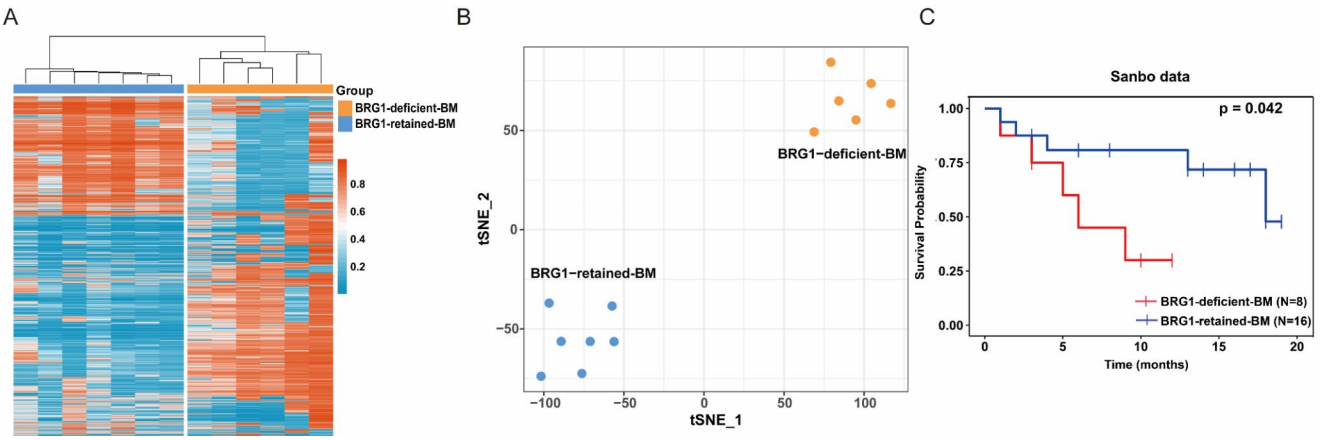

Fig. 3 Brain-metastatic lung adenocarcinoma with BRG1 deficiency and a poorer prognosis has unique methylation characteristics. (**A**-**B**) unsupervised clustering heatmap and t-SNE plot of the two cohorts reveal distinct methylome clusters. (**C**) Overall survival curves were estimated using the Kaplan-Meier method. Sanbo data illustrated that BRG1-deficient BM cohort had a worse prognosis

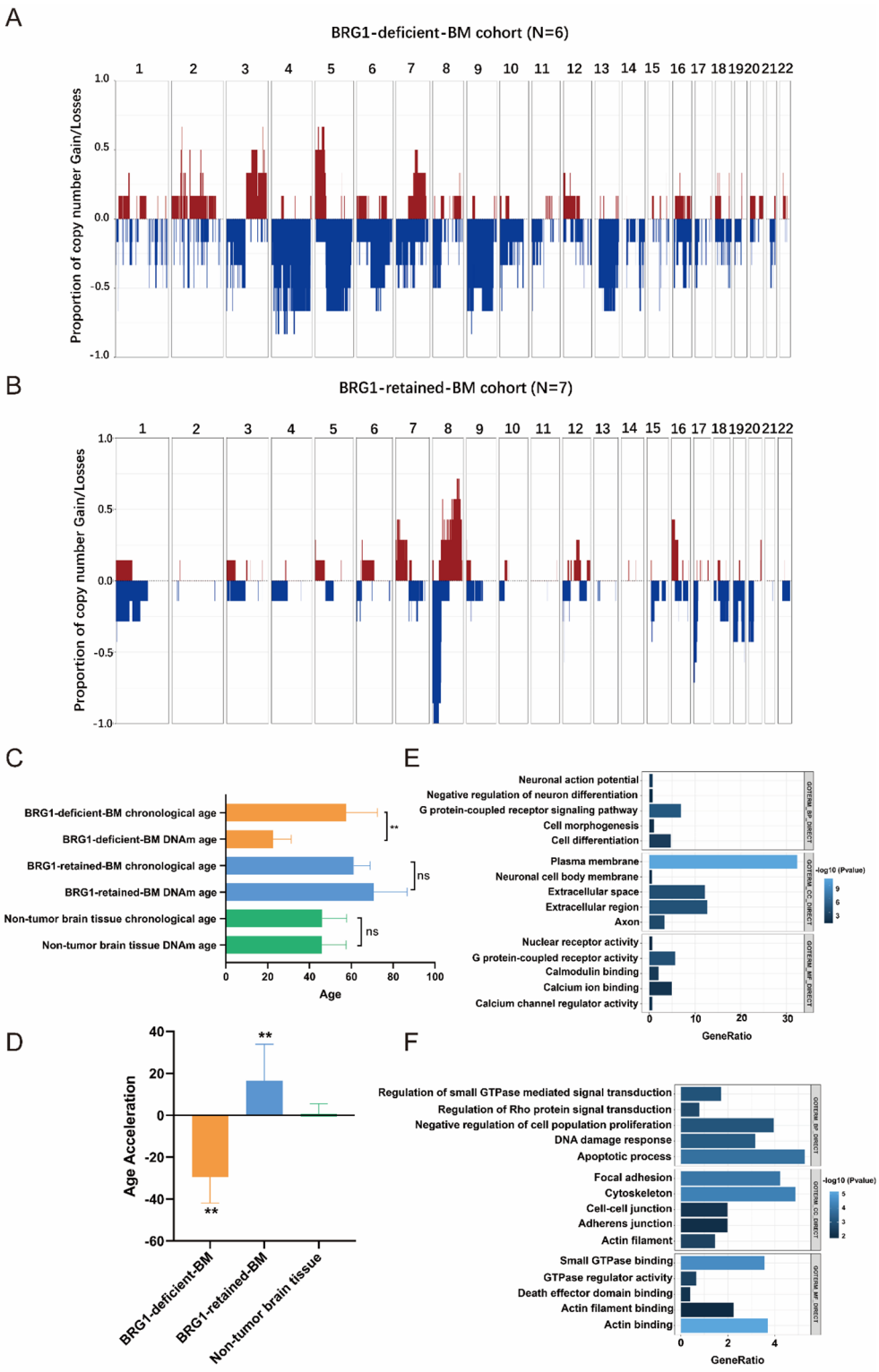

Fig. 4 BRG1-deficient BM cohort has high-frequency genomic instability and low DNA methylation age. Copy number profiles showing the genetic variations in BRG1-deficient BM cohort **(A)** and BRG1-retained BM cohort **(B)**. BRG1-deficient BM cohort **(A)** has more chromosomal instability including loss of chromosomes 4, 5, 6, and 9. BRG1-retained BM cohort **(B)** has loss of chromosome 8p and gain of chromosome 8q. (**C**) BRG1-deficient BM cohort has significantly lower DNA methylation age compared with chronologic age. (**D**) Age acceleration in three samples groups. BRG1-deficient samples have decreased age acceleration. (**E and F**) Top 5 most significant gene ontology categories enriched in the hypermethylated and hypomethylated DMPs

BRG1-deficient BM group. However, in the BRG1-retained BM group, there were 10 samples with Ki-67 positivity greater than 30% (10 /16) (Table 2). These results indicate that, compared to the BRG1-retained BM cohort, the BRG1-deficient BM cohort exhibits higher tumor proliferation indices.

We further identified differentially methylated positions (DMPs) between BRG1-deficient BM cohort, BRG1-retained BM cohort, and non-tumor brain tissue (NTB) in

our data. Gene ontology analysis was separately performed in the hypermethylated and hypomethylated DMPs. In the BRG1-deficient BM cohort and BRG1-retained BM cohort, the hypomethylation of differentially methylated regions was primarily enriched in negative regulation of neuron differentiation, G protein-coupled receptor signaling pathway and cell differentiation (Fig. 4E and Supplemental Table S3). The hypermethylation of differentially methylated region was regulation of small GTPase mediated signal transduction, regulation of Rho protein signal transduction, DNA damage response, and apoptotic process (Fig. 4F and Supplemental Table S3).

In BRG1-deficient BM cohort and NTB cohort, hypermethylated DMPs were enriched in cell migration, cytoskeleton, and small GTPase binding (Supplemental Fig. S3A and Supplemental Table S3). Hypomethylated DMPs were enriched in cell-cell signaling and cytoskeleton (Supplemental Fig. S3B and Supplemental Table S3). In BRG1-retained BM cohort and NTB cohort, hypermethylated DMPs were enriched in cell differentiation and actin cytoskeleton organization (Supplemental Fig. S3C and Supplemental Table S3). Hypomethylated DMPs were enriched in regulation of Rho protein signal transduction and cell migration (Supplemental Fig. S3D and Supplemental Table S3). All of these functional enrichment analyses were associated with metastatic cancer.

These findings indicate that the rare instances of lung adenocarcinoma with brain metastasis that exhibit BRG1 deficiency are marked by genomic instability, a signature of low methylation age, involved in negative regulation of neuron differentiation, G protein-coupled receptor signaling pathway, regulation of Rho protein signal transduction, DNA damage response, and apoptotic process. All of which are indicative of aggressive proliferative characteristics in these specimens.

Discussion

The lack of effective therapeutic options for LUAD patients with brain metastasis remains a significant concern [43–45]. Accurate diagnosis and treatment options for lung adenocarcinoma with brain metastasis were few and limited in their efficacy. In the present investigation, we conducted a comprehensive analysis of 25 LUAD-BM samples, encompassing clinical, histopathological, and molecular appraisals, with subsequent DNA methylation sequencing data analysis performed on a subset of 13 samples. Based on the status of BRG1, the samples were primarily divided into two groups. Through the analysis of multi-omics data, the study ultimately identified a rare subtype of lung adenocarcinoma brain metastasis, characterized by the absence of BRG1. In lung cancer, inactivation of the catalytic subunit SMARCA4 (BRG1) is the most common alteration within the SWI/SNF complex and has been associated with poor patient outcomes [46, 47]. However, in LUAD-BM samples, samples with deletion of BRG1 protein were rare. These patients have a significantly worse prognosis. This study was the first to cluster samples based on DNA methylation data under unsupervised clustering conditions. We defined this group of patients as the BRG1-deficient BM group.

Clinical characteristics of BRG1-deficient BM group was significantly associated with male sex and smoking history. However, given the limitations imposed by the sample size, the findings necessitate further validation through the incorporation of a larger cohort. The group of samples was further explored in depth by molecular marker diagnostics and molecular genetic characterization. Immunohistochemical staining shows that BRG1 was absent along with the deletion of TTF1 and NapsinA. Regarding the molecular characteristics in the BRG1-deficient BM group, samples have high frequency of SMARCA4 and TP53 mutation. More abundant CNVs were observed in BRG1-deficient BM group, suggesting that this group had stronger genomic instability, which was in accordance with the hypothesis that large-scale genomic alterations, such as copy number changes, is often evident at metastatic sites and genomic instability drives tumor progression and metastasis [48]. On the other hand, research indicates that TP53 mutations are associated with low DNA methylation age. Similar to normal cells, the DNAm age of cancer cells increases with propagation, which indicates that cancer cells with lower DNAm age have higher potential to proliferate and thus might grow into more aggressive tumors [27]. The low DNAm age was found in this group. The results indicate that this group of samples has significant proliferative potential. However, the mechanism underly this association remains unknown.

Due to the limited sample size of this study and the fact that the mechanism of disease progression in the BRG1deficient BM group was not explored in depth, in the future, with the continuous and in-depth study of this group of disease types, we will further search for precise therapeutic targets and strategies for this type of disease.

Collectively, our dataset and accompanying classification scheme proposed here advance LUAD-BM diagnostics from histology alone to an integrated profiling combining histology and molecular markers, with the potential for higher accuracy of risk assessment for individual patients. This study combines traditional pathologic diagnosis with DNA methylation classification prediction to provide an adjunctive role in the accurate diagnosis of LUAD-BM.

Supplementary Information The online version contains supplementary material available at https://doi.org/10.1007/s10585-025-10337-2.

Acknowledgements Not applicable.

Author contributions X.Q., J.Y, and J.F. conceived the Study Conception and designed the experiments; L.X., W.Z., M.Z., Ze.D., Z.H., and M.Z. provided the Sample Resources. J.F., Ze.D., and X.L. performed the experiments and collected the data. J.Y and J.F. participated in the analysis of the results.J.Y., and J.F. wrote and revised the paper.

Funding None.

Data availability Sequence data that support the findings of this study have not been deposited in a public repository because of institutional ethical restrictions. The requestors could complete a data request and when contacting the corresponding author (xszqxl169@mail.ccmu.edu.cn) details on data sharing criteria for requesting access will be sent.

Declarations

Ethics approval and consent to participate Approval for conducting this study was obtained from the institutional ethics committee at Sanbo Brain Hospital, Capital Medical University and Beijing Neurosurgical Institute, Capital Medical University Written informed consent was obtained from all patients and/or their legal representatives.

Consent for publication Not applicable.

Competing interests The authors declare no competing interests.

References

1. Mardinian K, Adashek JJ, Botta GP, Kato S, Kurzrock R (2021) Implications of an altered Chromatin-Remodeling gene for cancer development and therapy. Mol Cancer Ther 20(12). https://doi.org/10.1158/1535-7163.Mct-21-0433
2. Wilson BG, Roberts CWM (2011) SWI/SNF nucleosome remodellers and cancer. Nat Rev Cancer 11(7):481–492. https://doi.org/10.1038/nrc3068
3. Tian YM, Xu L, Li X, Li HM, Zhao MF (2023) SMARCA4: Current status and future perspectives in non-small-cell lung cancer. Cancer Lett. 554. https://doi.org/ARTN2160221016/j.canlet.2022.216022
4. Armon S, Hofman P, Ilié M (2021) Perspectives and Issues in the Assessment of Deficiency in the Management of Lung Cancer Patients. Cells-Basel. 10(8). https://doi.org/ARTN19203390/cells10081920
5. Naito T, Udagawa H, Umemura S et al (2019) Non-small cell lung cancer with loss of expression of the SWI/SNF complex is associated with aggressive clinicopathological features, PD-L1-positive status, and high tumor mutation burden. Lung Cancer 138:35–42. https://doi.org/10.1016/j.lungcan.2019.10.009
6. Concepcion CP, Ma S, LaFave LM et al (2022) Inactivation promotes Lineage- specific transformation and early metastatic features in the lung. Cancer Discov 12(2):562–585. https://doi.org/10.1158/2159-8290.Cd-21-0248
7. Pedrosa RMSM, Mustafa DAM, Aerts JGJV, Kros JM (2018) Potential Molecular Signatures Predictive of Lung Cancer Brain Metastasis. Front Oncol. 8. https://doi.org/ARTN1593389/fonc.2018.00159
8. Wanleenuwat P, Iwanowski P (2020) Metastases to the central nervous system: molecular basis and clinical considerations. J Neurol Sci 412:116755. https://doi.org/10.1016/j.jns.2020.116755
9. Cagney DN, Martin AM, Catalano PJ et al (2017) Incidence and prognosis of patients with brain metastases at diagnosis of systemic malignancy: a population-based study. Neurooncology 19(11):1511–1521. https://doi.org/10.1093/neuonc/nox077
10. Capper D, Jones DTW, Sill M et al (2018) DNA methylation-based classification of central nervous system tumours. Nature 555(7697):469–. https://doi.org/10.1038/nature26000
11. Koelsche C, Schrimpf D, Stichel D et al (2021) Sarcoma classification by DNA methylation profiling. Nat Commun 12(1):498. https://doi.org/ARTN1038/s41467-020-20603-4
12. Sahm F, Schrimpf D, Stichel D et al (2017) DNA methylation-based classification and grading system for meningioma: a multicentre, retrospective analysis. Lancet Oncol 18(5):682–694. https://doi.org/10.1016/S1470-2045(17)30155-9
13. Network CGAR (2014). Comprehensive molecular profiling of lung adenocarcinoma Nature. 2018; 511(7715):543–559. https://doi.org/10.1038/s41586-018-0228-6
14. Sandoval J, Mendez-Gonzalez J, Nadal E et al (2013) A prognostic DNA methylation signature for stage I Non-Small-Cell lung cancer. J Clin Oncol 31(32):4140–. https://doi.org/10.1200/Jco.2012.48.5516
15. Shinjo K, Okamoto Y, Takeuchi I et al (2012) Integrated analysis of genetic and epigenetic alterations reveals CpG Island methylator phenotype associated with distinct clinical characters of lung adenocarcinoma. Cancer Res 72. https://doi.org/10.1158/1538-7445.Am2012-5003
16. Yang Z, Yang N, Ou QX et al (2018) Investigating novel resistance mechanisms to Third-Generation EGFR tyrosine kinase inhibitor osimertinib in Non-Small cell lung cancer patients. Clin Cancer Res 24(13):3097–3107. https://doi.org/10.1158/1078-0432.Ccr-17-2310
17. Bolger AM, Lohse M, Usadel B (2014) Trimmomatic: a flexible trimmer for illumina sequence data. Bioinformatics 30(15):2114–2120. https://doi.org/10.1093/bioinformatics/btu170
18. Li H, Durbin R (2009) Fast and accurate short read alignment with Burrows-Wheeler transform. Bioinformatics 25(14):1754–1760. https://doi.org/10.1093/bioinformatics/btp324
19. DePristo MA, Banks E, Poplin R et al (2011) A framework for variation discovery and genotyping using next-generation DNA sequencing data. Nat Genet 43(5):491–498. https://doi.org/10.1038/ng.806
20. Koboldt DC, Zhang QY, Larson DE et al (2012) VarScan 2: somatic mutation and copy number alteration discovery in cancer by exome sequencing. Genome Res 22(3):568–576. https://doi.org/10.1101/gr.129684.111
21. Newman AM, Bratman SV, Stehr H et al (2014) FACTERA: a practical method for the discovery of genomic rearrangements at breakpoint resolution. Bioinformatics 30(23):3390–3393. https://doi.org/10.1093/bioinformatics/btu549

22. Shen RL, Seshan VE (2016) FACETS: allele-specific copy number and clonal heterogeneity analysis tool for high-throughput DNA sequencing. Nucleic Acids Res 44(16). https://doi.org/ARTN1093/nar/gkw520 e131
23. Aryee MJ, Jaffe AE, Corrada-Bravo H et al (2014) Minfi: a flexible and comprehensive bioconductor package for the analysis of infinium DNA methylation microarrays. Bioinformatics 30(10):1363–1369. https://doi.org/10.1093/bioinformatics/btu049
24. Feng J, Duan ZJ, Yao K et al (2023) Primary papillary epithelial tumor of the Sella and posterior pituitary tumor show similar (epi) genetic features and constitute a single neuro-oncological entity. Neurooncology 25(8):1487–1497. https://doi.org/10.1093/neuonc/noad067
25. Chakrayarthy A, Furness A, Joshi K et al (2018) Pan-cancer deconvolution of tumour composition using DNA methylation. Nat Commun. 2018(9):3220–9. https://doi.org/ARTN464211038/s41467-018-07155-4
26. Zhang W, Xu H, Qiao R et al (2022) ARIC: accurate and robust inference of cell type proportions from bulk gene expression or DNA methylation data. Brief Bioinform 23(1). https://doi.org/10.1093/bib/bbab362
27. Horvath S (2015) Erratum to: DNA methylation age of human tissues and cell types. Genome Biol 16(1):96. https://doi.org/10.1186/s13059-015-0649-6
28. Tian Y, Morris TJ, Webster AP et al (2017) ChAMP: updated methylation analysis pipeline for illumina beadchips. Bioinformatics 33(24):3982–3984. https://doi.org/10.1093/bioinformatics/btx513
29. Huang da W, Sherman BT, Lempicki RA (2009) Systematic and integrative analysis of large gene lists using DAVID bioinformatics resources. Nat Protoc 4(1):44–57. https://doi.org/10.1038/nprot.2008.211
30. Capper D, Stichel D, Sahm F et al (2018) Practical implementation of DNA methylation and copy-number-based CNS tumor diagnostics: the Heidelberg experience. Acta Neuropathol 136(2):181–210. https://doi.org/10.1007/s00401-018-1879-y
31. Skidmore ZL, Wagner AH, Lesurf R et al (2016) GenVisR: genomic visualizations in R. Bioinformatics 32(19):3012–3014. https://doi.org/10.1093/bioinformatics/btw325
32. Dagogo-Jack I, Schrock AB, Kem M et al (2018) Clinicopathologic characteristics and molecular features of BRG1-deficient non-small cell lung cancer (NSCLC). J Clin Oncol 36(15). https://doi.org/10.1200/JCO.2018.36.15_suppl.12083
33. Schoenfeld AJ, Montecalvo J, Namakydoust A et al (2020) The genomic landscape of SMARCA4 alterations and association with patient outcomes in lung cancer. J Thorac Oncol 15(2):S14–S14
34. Fernando TM, Piskol R, Bainer R et al (2020) Functional characterization of variants identified by targeted exome-sequencing of 131,668 cancer patients. Nat Commun. 11(1). https://doi.org/ARTN55511038/s41467-020-19402-8
35. Schmid S, Solomon DA, Perez E et al (2021) Genetic and epigenetic characterization of posterior pituitary tumors. Acta Neuropathol 142(6):1025–1043. https://doi.org/10.1007/s00401-021-02377-1
36. Figueroa ME, Lugthart S, Li YS et al (2010) DNA methylation signatures identify biologically distinct subtypes in acute myeloid leukemia. Cancer Cell 17(1):13–27. https://doi.org/10.1016/j.ccr.2009.11.020
37. Goeppert B, Toth R, Singer S et al (2019) Integrative analysis defines distinct prognostic subgroups of intrahepatic cholangiocarcinoma. Hepatology 69(5):2091–2106. https://doi.org/10.1002/hep.30493
38. Pan H, Wang H, Zhang X, Yang F, Fan X, Zhang H (2022) Chromosomal instability-associated MAT1 LncRNA insulates MLL1-guided histone methylation and accelerates tumorigenesis. Cell Rep 41(11). https://doi.org/10.1016/j.celrep.2022.111829
39. Esteller M, Herman JG (2002) Cancer as an epigenetic disease: DNA methylation and chromatin alterations in human tumours. J Pathol 196(1):1–7. https://doi.org/10.1002/path.1024
40. Bocklandt S, Lin W, Sehl ME et al (2011) Epigenetic predictor of age. PLoS ONE 6(6). https://doi.org/ARTN1371/journal.pone.0014821 e14821
41. Koch CM, Wagner W (2011) Epigenetic-aging-signature to determine age in different tissues. Aging-Us 3(10):1018–1027. https://doi.org/10.18632/aging.100395
42. Horvath S, Garagnani P, Bacalini MG et al (2015) Accelerated epigenetic aging in down syndrome. Aging Cell 14(3):491–495. https://doi.org/10.1111/acel.12325
43. Steeg PS, Camphausen KA, Smith QR (2011) Brain metastases as preventive and therapeutic targets. Nat Rev Cancer 11(5):352–363. https://doi.org/10.1038/nrc3053
44. Lin XL, DeAngelis LM (2015) Treatment of brain metastases. J Clin Oncol 33(30):3475–. https://doi.org/10.1200/Jco.2015.60.9503
45. Jiang JL, Wu LH, Yuan F et al (2020) Characterization of the immune microenvironment in brain metastases from different solid tumors. Cancer Med-Us 9(7):2299–2308. https://doi.org/10.1002/cam4.2905
46. Rekhtman N, Montecalvo J, Chang JC et al (2020) SMARCA4-Deficient thoracic sarcomatoid tumors represent primarily Smoking-Related undifferentiated carcinomas rather than primary thoracic sarcomas. J Thorac Oncol 15(2):231–247. https://doi.org/10.1016/j.jtho.2019.10.023
47. Helming KC, Wang XF, Roberts CWM (2014) Vulnerabilities of mutant SWI/SNF complexes in cancer. Cancer Cell 26(3):309–317. https://doi.org/10.1016/j.ccr.2014.07.018
48. Bakhoum SF, Ngo B, Laughney AM et al (2018) Chromosomal instability drives metastasis through a cytosolic DNA response. Nature 553(7689):467–. https://doi.org/10.1038/nature25432